ISSN 1990-7931, Russian Journal of Physical Chemistry B, 2018, Vol. 12, No. 4, pp. 669–676. © Pleiades Publishing, Ltd., 2018.
Original Russian Text © A.A. Chesnokov, S.E. Kuratov, 2018, published in Khimicheskaya Fizika, 2018, Vol. 37, No. 8, pp. 43–51.

COMBUSTION, EXPLOSION, AND SHOCK WAVES

The Numerical Simulation of Indirect Laser Radiation on Pentaerythritol Tetranitrate

A. A. Chesnokov[a], * and S. E. Kuratov[a]

[a] *Dukhov Research Institute of Automatics, Moscow, Russia*

**e-mail: syfjet@gmail.com*

Received August 23, 2017

Abstract—This paper analyzes detonation processes in an explosive laser device, in particular the indirect radiation of an explosive material. A hydrodynamic approach is applied to the numerical analysis, the results of which are in good agreement with experimental data.

Keywords: laser ignition, PETN, hydrodynamics, thin metal films, numerical simulation

DOI: 10.1134/S1990793118040206

INTRODUCTION

The use of thin metal films in experiments on loser ignition of explosive substances (ESs) is directed to minimization of their ignition energy. In this way, [1] presented the results of pentaerythritol tetranitrate (PETN) ignition using a neodymium laser with a radiation wavelength of 1.06 μm and a pulse duration of 30–50 ns. Experiments were carried out in both direct irradiation of an ES and using an intermediate metal film of manganese covering the transparent glass window on the ES side.

The study [2] was devoted to researching ignition of PETN with dispersity of 8000 $cm^2\ g^{-1}$ and density of 0.9 $g\ cm^{-3}$, using various metal films: aluminum, manganese, copper, zinc, magnesium, and lead. The laser used in the experiments was similar to that used in [1]. It was shown that the dependencies of threshold ignition energy of PETN on thickness of film are qualitatively similar for all the considered metals. The same authors studied the optical characteristics of metal films, including their coefficients of absorption, reflection, and transmission [3].

The authors of [4] considered the laser ignition of PETN in statement of direct irradiation, using a neodymium laser with a modulated quality factor. That study included several experiments where an aluminum film with a thickness of 0.5 μm was sprayed on a transparent window in order to amplify plasma formation on the ES/window boundary

The work [5] describes experiments on the indirect irradiation of PETN by laser pulse with energies of 80–150 mJ and durations of 12 and 4 ns. The thickness of the aluminum film was varied from 100 to 300 nm.

There have been numerous theoretical studies of heat conductivity and kinetics equations, but few studies have used a hydrodynamic approach. The solution of the heat conductivity problem [6–9] allows for the analysis of the initial stages of the laser ignition process, i.e., warming an ES with further chemical decomposition, as described by the Arrhenius equation. This approach can be applied to the consideration of the microscopic problems of warming an ES in the contact of the ES with admixture [6] or, in the case of interaction of radiation with a high-density pure ES [7]. However, in the application to formation of the detonation wave and especially in a porous ES, a heat-conductivity approach becomes meaningless because it is not able to describe the given process.

Among the presently existing hydrodynamic methods for solving problems of the direct interaction of laser radiation with an ES, [10], which described the simulation of the detonation ignition of pure PETN, should be noted; however, it lacks a detailed quantitative comparison of the results obtained with experimental data [11] considers the inflammation of octogen by a CO_2 laser and presents an analysis of the flame propagation process. Theoretical studies of the indirect irradiation of ESs include work [12], which contains only a statement of one-dimensional computation, as well as work [13], where a solution is presented to a statement of heat conductivity with no comparison with experimental data.

This work performed a numerical simulation of the ignition of PETN decomposition using thin metal films of aluminum within the framework of the experimental statements of work [2].

PHYSICAL-MATHEMATICAL MODEL

Studies of the indirect laser ignition of ESs involve constructions (Fig. 1) consisting of body (plexiglass

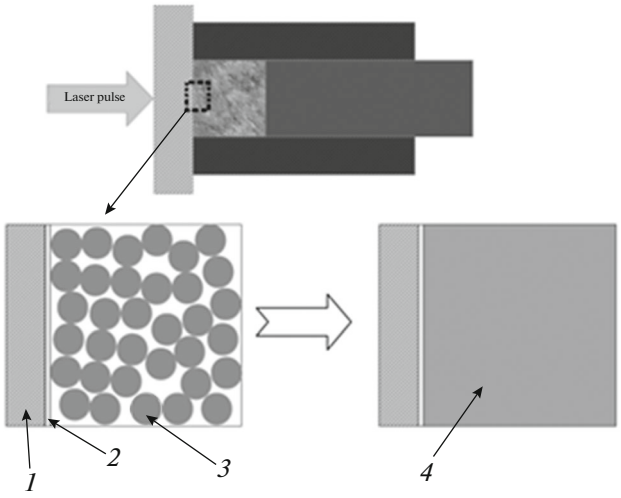

Fig. 1. Schematic image of experimental assembly and mesoscopic structure of the ES and its continual approximation: (*1*) glass, (*2*) metal film, (*3*) ES crystals, (*4*) simulated continuum.

with inner diameter of 3 mm), transparent base surface (glass with a thickness of about 1 mm) with a sprayed metal film 1 nm thick and ES PETN with a height and diameter of 3 mm. The assembly is targeted by a generated laser pulse with a radiation wavelength of 1.06 μm.

The metal film evaporates as it absorbs radiation. The sharp pressure and temperature jump in the region of the film region generate shock waves propagating through the ES and the bare glass surface. Chemical decomposition begins after the front of the shock wave reaches the ES, and depending on experimental conditions, a detonation wave is formed in the ES. The presence of the optical window in the assembly prevents early projection of film substance into free space and thereby provides the decreases into the laser pulse energy required for ignition of ES [1, 14].

The experiment under consideration is at the intersection of optics, plasma physics, and explosion physics; thus to simulate it, one has to take processes with essentially different temporal and spatial scales into account. This makes the simulation problem extremely complicated and hard-to-solve.

In this work we apply a continual hydrodynamic method, which was previously used to study the direct irradiation of the ES [15], which includes various phenomenological models of compaction, chemical decomposition, and other processes. Though this approach significantly simplifies the description of various physico-chemical mechanisms, it allows the understanding of what takes place in experiments.

A general view of the hydrodynamics equations for single spatial variable in Lagrangian formulation is shown below [16, 17]:

$$\frac{dM}{dt} = 0, \quad \frac{du}{dt} + V\frac{\partial P}{\partial z} = 0, \quad \frac{de}{dt} + P\frac{\partial V}{\partial t} = QV, \quad \frac{dz}{dt} = u, \quad P = P(\rho, e), \tag{1}$$

where t is time, z is a spatial variable, M is the mass of the medium, V is the partial volume of the medium element, u is velocity, P is pressure, e is internal energy, ρ is density of element, and Q is external source of energy.

First, three equations define mass, pulse and energy conservation laws, a fourth equation allows the computation of motion trajectories of medium elements, and the last equation establishes a connection between pressure, density and internal energy of the substance (substance state equation (SE)). For the simulation we are confined to one-dimensional approximation.

The interaction of laser radiation with non-transparent media, such as metals for a wide range of electromagnetic waves, is reduced to the reflection and scattering of light by the surface, as well as its absorption in a very thin surface screen-layer. This leads to strong heating, melting, and evaporation of substance and ionization of the obtained vapors, i.e., to plasma formation [18, 19].

Theoretical studies of physical processes appearing during the interaction of laser radiation with substance, such as ionization, the formation of a plasma flame, and others, require using corresponding models, which significantly complicate the solution of the stated problem. For this reason, in this work we exclusively consider the thermal effects of the impact of the laser pulse. This approximation allows us to simulate the process of interaction between laser radiation and metal films by introducing an external, non-stationary source of energy [18, 20]:

$$Q = \frac{WA}{\sqrt{\pi}\delta\tau} e^{-(t/\tau)^2} e^{-(z/\delta)}, \tag{2}$$

where W, τ, A, δ are the density of energy, half-width of pulse duration. and the coefficient and depth of absorption, respectively [3, 21, 22].

Let us estimate the distribution of energy by thickness of plate from elementary considerations within the frameworks of heat conductivity approach. It is known that distance passed by thermal wave can be estimated as $x \sim (\chi t)^{1/2}$, where χ is the temperature conductivity coefficient [23]. Over the course of a pulse duration of 40 ns, this distance corresponds to a quantity of order of 2 μm, which is an order of magnitude greater than the characteristic thicknesses of films considered in the experiment. This allows the consideration of the interaction of laser radiation with the substance in an approximation of uniform heating. As a result, formula (2) can be simplified:

$$Q = \frac{WA}{h\tau\sqrt{\pi}} e^{-(t/\tau)^2}, \quad (3)$$

where h is the thickness of the film.

It is necessary to note that for film thicknesses $h \approx \delta$, radiation begins penetrating into ES domain and the problem is switched to case of direct irradiation of ES, which was considered in work [15]. However, in this work, the assumption of non-transparent film is used.

As mentioned above, the impact of laser pulse on metal film leads to various phase transitions in metal, which are taken into account using a wide-range Tillotson substance state equation [24]:

$$\begin{cases} P_1 = A\mu + B\mu^2 + \left(a + \dfrac{b}{w_0}\right)\rho e, \quad \mu \geq 0, \\ P_2 = A\mu + \left(a + \dfrac{b}{w_0}\right)\rho e, \quad \mu < 0, \quad e < e_s, \\ P_3 = P_2 + \dfrac{(P_4 - P_2)(e - e_s)}{(e_{sd} - e_s)}, \quad \mu < 0, \quad e_s \leq e < e_{sd}, \\ P_4 = a\rho e + \left(\dfrac{b\rho e}{w_0} + A\mu e^{\beta\eta}\right)e^{-\alpha\eta^2}, \quad \mu < 0, \quad e \geq e_{sd}. \end{cases} \quad (4)$$

$$w_0 = 1 + \frac{e}{e_0}\left(\frac{\rho_0}{\rho}\right)^2, \quad \mu = \frac{\rho}{\rho_0} - 1, \quad \eta = 1 - \frac{\rho_0}{\rho},$$

where $A, B, a, b, \alpha, e_{sd}, e_s, e_0, \beta$ are constants [25, 26].

This set includes four equations connected with each other by various conditions. Each allows for the description of the behavior of metal in a certain domain of phase diagram (Fig. 2). The first equation is responsible for the state of substance during compression, while the second considers its expansion. The fourth equation describes the substance in a gaseous state, and the third shows the intermediate state of medium, representing a link between the second and fourth equations.

The optical window of the detonator was described using elastic state equation:

$$P = \rho_0 c_0^2 \left(\frac{\rho}{\rho_0} - 1\right), \quad (5)$$

where $\rho_0 = 2650$ kg m^{-3}, $c_0 = 4800$ m s^{-1} [10].

The energy-yielding material is considered in the form of a substance consisting of two different phases: non-aggregated solid substance (the sol index) and its gaseous products of chemical reaction (the gas index). The mechanics of heterogeneous environments allow each phase its own series of characteristics (pressure, internal energy, density, velocity, etc.) and is described by its own set of hydrodynamic equations [20]. Various simplifications are applied to study the behavior of multiphase environment [27, 28].

In this work, we use equality conditions for phase velocities ($u = u_{sol} = u_{gas}$, $v = v_{sol} = v_{gas}$), pressures ($P = P_{sol} = P_{gas}$), and additivity conditions for internal energy ($e = (1 - \alpha)e_{gas} + \alpha e_{sol}$, where α is the mass fraction of the solid phase). These conditions, leading to the homogenization the of multiphase environment, allow the simulation of the behavior of an ES within the frameworks of equation set (1).

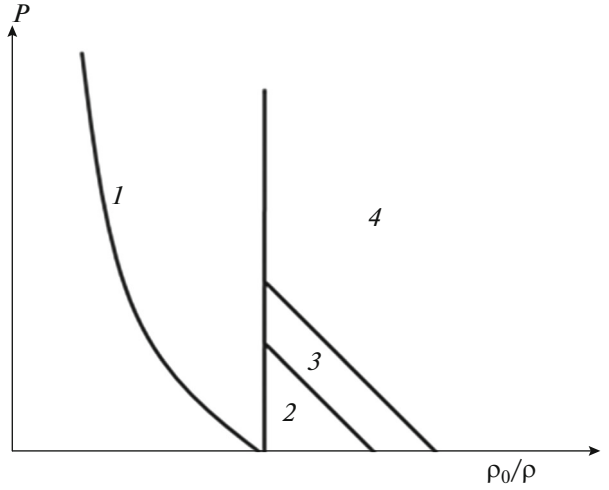

Fig. 2. Schematic image of phase diagram of Tillotson state equation: (*1*) compression domain, (*2*) tension domain, (*3*) transitional state, (*4*) gas medium.

The two last conditions allow state equation to be obtained for energy-yielding material, using two Jones–Wilkins–Lee equations for each phase, as in [20, 29]:

$$P = \{\rho_0 e + \alpha(F_{sol}[\rho_0/\rho_{sol}] - F_{sol}[1]) + (1 - \alpha) \times (F_{gas}[\rho_0/\rho_{gas}] + q)\}\left\{\frac{\alpha(\rho_0/\rho_{sol})}{\omega_{sol}} + \frac{(1 - \alpha)(\rho_0/\rho_{gas})}{\omega_{gas}}\right\},$$

$$F_{sol}[\chi] = A_{sol}\left(\frac{\chi}{\omega_{sol}} - \frac{1}{R_1^{sol}}\right)e^{-R_1^{sol}\chi} + B_{sol}\left(\frac{\chi}{\omega_{sol}} - \frac{1}{R_2^{sol}}\right)e^{-R_2^{sol}\chi}, \quad (6)$$

$$F_{gas}[\chi] = A_{gas}\left(\frac{\chi}{\omega_{gas}} - \frac{1}{R_1^{gas}}\right)e^{-R_1^{gas}\chi} + B_{gas}\left(\frac{\chi}{\omega_{gas}} - \frac{1}{R_2^{gas}}\right)e^{-R_2^{gas}\chi}.$$

where ρ_{sol} and ρ_{gas} are real densities of ES and its explosion products, $\rho_0 = 1750$ kg m^{-3}, $A_{sol} = 3748$ GPa, $B_{sol} = -131.3$ GPa, $R_1^{sol} = 7.2$, $R_2^{sol} = 3.6$, $\omega_{sol} = 1.173$, $A_{gas} = 617$ GPa, $B_{gas} = 16.926$ GPa, $R_1^{gas} = 4.4$, $R_2^{gas} = 1.2$, $\omega_{gas} = 0.25$, and $q = 10.1$ GPa [30].

The correlation between the average density of the environment and the real value of the density of solid substances and its products is defined by formulas [31]:

$$\rho_{sol} = \frac{\alpha}{\beta}\rho, \quad \rho_{gas} = \frac{1-\alpha}{1-\beta}\rho. \tag{7}$$

where β is the volume fraction of the ES.

Since the ES may be subject to chemical transformations, the equation set must be supplemented by a kinetics equation. Accounting the fact that the energy-yielding material in the explosive assemblies is a porous medium, equation set must also be supplemented by a deformation model of porous media [32]. In this work, we used the kinetics of ES decomposition and compaction model suggested in work [33], which were elaborated for describing a transition of burning into detonation and were calibrated over a wide range of PETN densities; however, they do not include parameters characterizing the dispersiveness of ES:

$$\begin{gathered}\frac{d\alpha}{dt} = -H(P - P_{ign})k_\alpha(P/P_{CJ})^\mu(\alpha)^\nu,\\ k_\alpha(\beta_0) = d_1\exp(a_1\beta_0^2 - b_1\beta_0 + c_1),\\ \mu(\beta_0) = a_2\beta_0^2 - b_2\beta_0 + c_2,\\ F = k_\beta(P - P_h)\left\{1 - \left[\frac{\beta_0(1-\beta)}{\beta(1-\beta_0)}\right]^{1/2}\right\},\\ \frac{d\beta}{dt} = \frac{\rho}{\rho_{sol}}\frac{d\alpha}{dt} + F,\end{gathered} \tag{8}$$

where H is the Heaviside function, P_{ign} is the threshold pressure of 10^7 Pa [29], P_{CJ} is the pressure at the Chapman–Jouget point, k_α, μ are constants depending on initial porosity, $a_1, b_1, c_1, a_2, b_2, c_2, k_\beta, P_h, \nu$ are adjustable constants [33], F is the compaction velocity of substance, and β_0 is the initial volume fraction of ES. The last equation defines the connection between volume and mass fractions of solid phase of energy-yielding material in Lagrangian variables [28]. In this way, the equations considered above are sufficient to operate explosive assemblies within the hydrodynamic approach.

The equation set was solved using an explicit algorithm elaborated by analogy with the results of [16, 34, 35] without elastoplastic and heat conductivity models. The mesh was the same for all materials, i.e., the contact zones are ideal [36]. The condition of the free surface of the rigid wall can be imposed on the boundary of computation domain. Vector quantities are computed at mesh nodes and scalar quantities are defined in cell centers. The order of computations performed within a single temporal step can be represented as follows. At the first step, the partial volume of cells is computed, equations of compaction and chemical kinetics are solved. The next step is to compute the velocities of mesh nodes. Then the internal energy is defined taking external sources into account. The last step includes the computation of pressure using state equations of substances. The computation of one temporal step is finished. The correctness of the numerical scheme and the applied models for computing detonation of porous ES were checked by shock-wave tests, and their results were compared with experimental data [15].

COMPUTATION STATEMENT AND SIMULATION RESULTS

Computation was carried out in a one-dimensional statement, where the boundaries of computational domain were considered to be free surfaces. The sizes of the simulated domain constituted 300 μm, where 100 μm were allocated for glass base material and the rest 200 μm were distributed between the ES and the aluminum film.

In the dislocation domain of the metal, the film mesh was uniform, with a step of 2 nm. Because the characteristic sizes of the ES and glass are significantly greater than the region occupied by film, the mesh was condensed into ES and glass zones to accelerate computation. There were 5000 and 1000 cells for the ES and glass, respectively. One computation was carried out with double the amount of cells in the region of the ES and glass to test mesh independence.

The parameters that were varied in computations were the thickness of film (from 20 to 160 nm, with a step of 20 nm) and energy (from 20 to 30 mJ, with a step of 0.5 mJ). The duration of laser pulse was 40 ns (τ = 20 ns). The absorption coefficient was 0.6–0.7, and the absorption depth δ = 10 nm [21, 22]. The density of the ES was 900 kg m^{-3}.

Uniform heating of metal film causes its expansion, and as the SE of metal reaches critical points, the phase state of the substance changes. Waves leading to the compaction of the ES and its chemical decomposition propagate in both directions. As a result of the high pressure behind the front of the shock wave, the rate of chemical decomposition of the ES increases, and as a result the detonation wave is formed at a distance from impact focus.

Profiles of physical quantities (pressure, density, volume and mass fractions) for the development of detonation process in the system for an energy of 24.5 mJ and a thickness of film of 120 nm are shown in Figs. 3 and 4. A region with low density is observed in Fig. 4a for density profile (less than 10 kg m^{-3}) that is connected with transition of aluminum to a gaseous state and its expansion.

When the shock wave passes the ES, it is possible to observe an increase in the volume fraction behind its front without any change of mass fraction (compaction of porous substance), followed by a gradual decreasing of both the volume and mass fractions (chemical decomposition of the ES). By about 98 ns and at distance of 0.15 mm from the contact zone, we can observe growth of pressure with sharply decreasing (almost to zero) volume and mass fractions of the ES, which means the formation of a detonation wave. By 100 ns, two supersonic waves have begun propagating

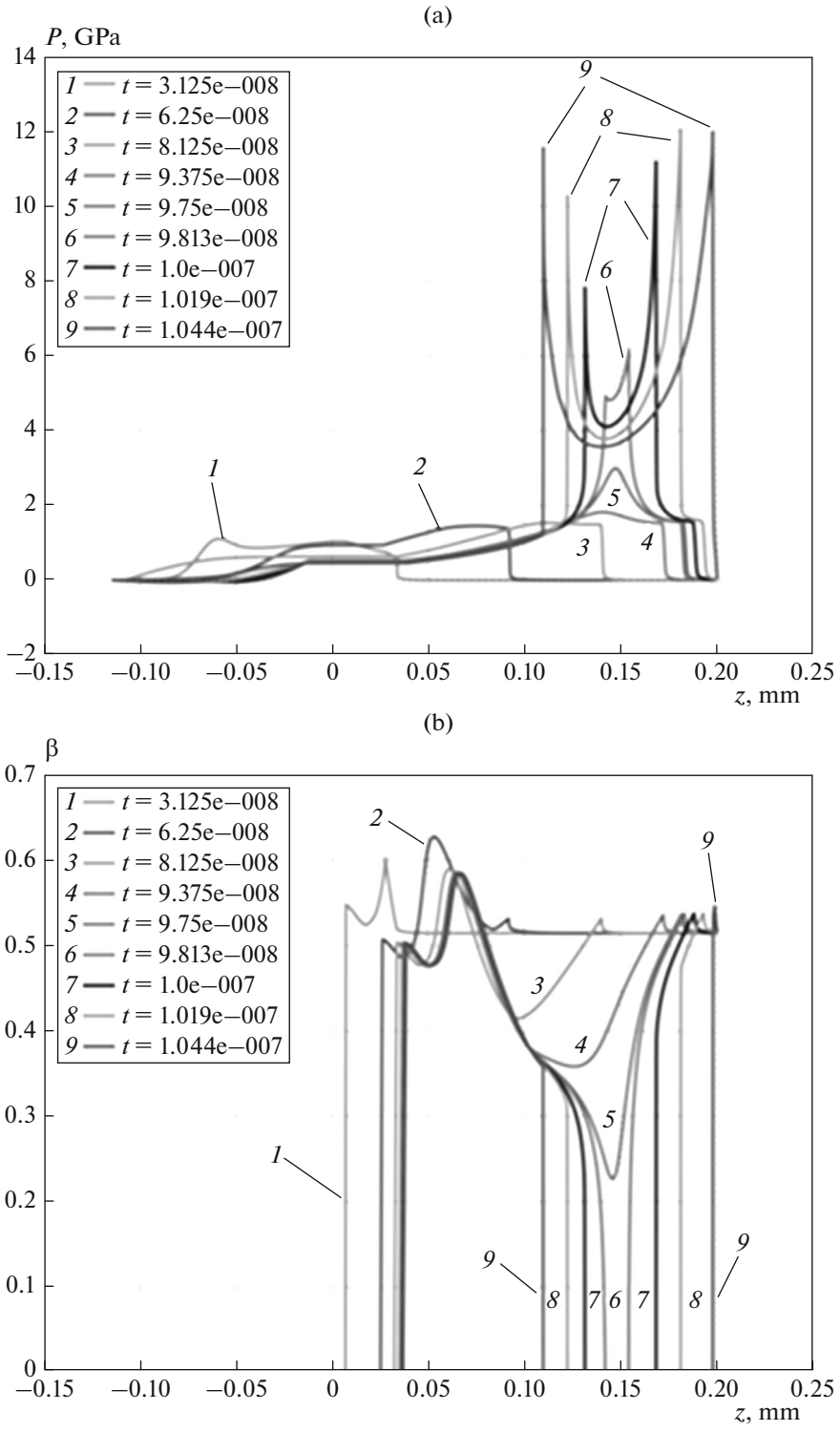

Fig. 3. Profiles of the pressure (a) and volume fraction (b) in the system at various moments of time.

through the ES: detonation and retonation [29, 33]. The velocity of the detonation wave at this moment of time is about 6.5 km s^{-1}, which is slightly greater than the experimental value [37]. This is connected with the fact that the detonation wave propagate through the ES, which was preliminarily compressed by the primary shock wave. By 104 ns, the velocity of the wave decreases to a value corresponding to those found in [15, 37].

The dependency of ignition energy on thickness of film is shown in Fig. 5, as recomputed by a formula

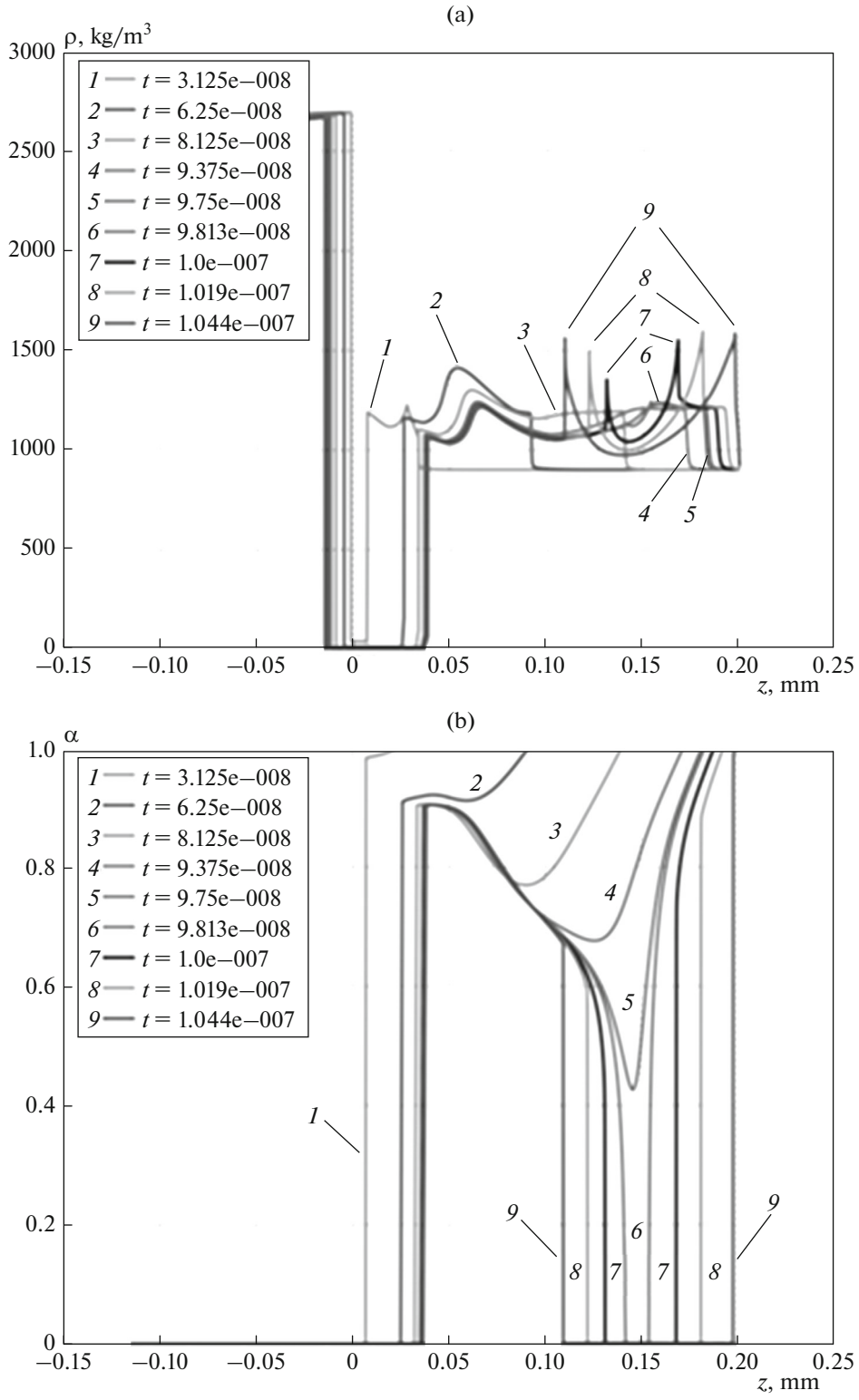

Fig. 4. Profiles of the density (a) and mass fraction (b) in the system at various moments of time.

coupling energy with the density of energy through the area of the laser spot $E = W\pi r^2$, where r is radius of the beam, 0.22 mm [2].

RESULTS AND DISCUSSION

The obtained character of the dependence of the threshold ignition energy is in qualitative agreement

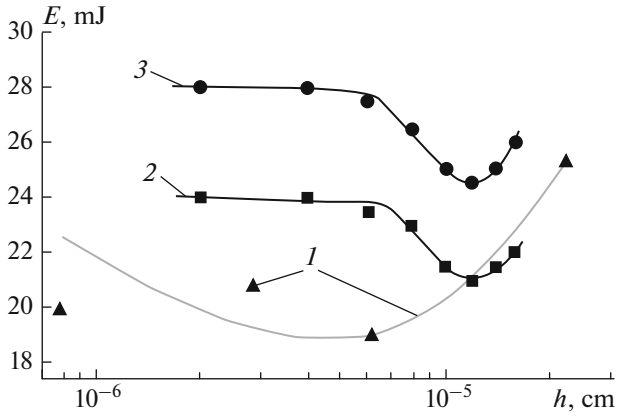

Fig. 5. Dependences of ignition energy on thickness of metal film: (*1*) experimental data and its approximation [2]; (*2*) computed curve with points of detonation ignition for absorption coefficient, which is 0.6; (*3*) computed curve with radiation coefficient, which is 0.7. The radius of the laser beam is 0.44 mm, and pulse duration is 40 ns.

with experimental data. The growth of ignition energy for film thicknesses greater than the optimal value in Fig. 5 is connected with large power consumption for heating the material and its transition into gaseous state. The increase in energy resulting from smaller film thicknesses is connected with the fact that the film substance is heated rapidly but in turn is discharged and cools down very rapidly as it reaches a gaseous state.

Within the selected approximations, experimental data and numerical computations are in good agreement. A satisfactorily agreement between the minimum energies of the computed and experimental curves (around 30%) was achieved; however, there is difference in optimal film thickness (by a factor of two). The variation of the absorption coefficient showed a significant impact on the result: an increment of 0.1 (to 0.7) decreases the threshold energy, on average, by 5 mJ.

It is known from experiments in [21] that optical depth increases to 40 nm a boiling temperature is reached, but this was not taken into account during simulation. It is necessary to note that a one-dimensional statement of continual approximation does not allow the computation of a projection of the film substance into the pores of the ES.

CONCLUSIONS

Study of the interactions between laser pulses and ESs and the analysis of different approaches to decreases the ignition threshold are current experimental and theoretical problems. The numerical simulation in the work was based on a physico-mathematical model that has been shown to successfully describe the direct laser ignition of PETN in optical assemblies and the shock-wave ignition of porous PETN [15, 20]. The given approach provided a qualitative and quantitative description for processes taking place during the indirect irradiation of ES by laser pulse and allowed the analysis of the dynamics of development of ES detonation process using phenomenological models for describing chemical decomposition and compaction.

A difference from an experiment with minimum energy of about 30% was obtained with a one-dimensional approximation, which is a good result at this point, but to obtain more complete idea of film projection, it is necessary to study the problem on a mesoscopic level, considering the compaction and burning of grains and the projection of metal film in more detail. Numerical and parametric studies have shown that detonation is highly influenced by the optical properties of metal film and especially the absorption coefficient.

REFERENCES

1. A. A. Volkova, A. D. Zinchenko, I. V. Sanin, et al., Fiz. Goreniya Vzryva, No. 5, 760 (1977).
2. V. I. Tarzhanov, A. D. Zinchenko, B. N. Smirnov, et al., Fiz. Goreniya Vzryva, No. 2, 111 (1996).
3. A. D. Zinchenko, V. I. Tarzhanov, V. I. Tokarev, et al., in *Rapid Explosive Initiation. Special Regimes of Detonation, Collection of Articles* (RFYaTs-VNIITF. Snezhinsk, 1998), p. 48 [in Russian].
4. L. C. Yang and V. J. Menichelli, Appl. Phys. Lett. **19** (11) (1971).
5. Y. Kotsuka, K. Nagayama, M. Nakahara, et al., Shock Waves **17**, 171 (2007).
6. I. G. Assovskiy and V. V. Kozynda, Dokl. Biochem. Biophys. **442**, 40 (2012).
7. A. V. Khaneft and V. A. Dolgachev, Combust. Explos., Shock Waves **50**, 105 (2014).
8. V. P. Tsiplev, E. Yu. Morozova, and A. S. Skripin, Izv. TPU **317**, 149 (2010).
9. L. Strakovkiy, A. Cohen, R. Fifer, et al., ARL-TR-1699 (Army Research Laboratory, 1998).
10. V. I. Tarzhanov, V. F. Kuropatenko, A. T. Sapozhnikov, et al., in *Proceedings of the Conference on Detonation, Critical Phenomena, Physicochemical Transformations in Shock Waves* (OIKhF AN SSSR, Chernogolovka, 1978), p. 46 [in Russian].
11. V. Meredith, L. Gross, and W. Beckstead, Combust. Flame **162**, 507 (2015).
12. S. Stewart, D. S. Saenz, J. A. Rodriguez, et al., in *Proceedings of the 13th International Detonation Symposium, Norfolk, VA, 2006,* p. 393.
13. A. V. Khaneft, V. A. Dolgachev, A. S. Zverev, and A. Yu. Mitrofanov, Combust., Explos. Shock Waves **52**, 91 (2016).
14. V. I. Tarzhanov, A. D. Zinchenko, V. I. Sdobnov, et al., Fiz. Goreniya Vzryva, No. 4, 113 (1996).
15. A. A. Chesnokov and S. E. Kuratov, Russ. J. Phys. Chem. B **12**, 83 (2018).

16. Ch. L. Mader, *Numerical Modeling of Detonations* (Univ. of California Press, Berkeley, Los Angeles, London, 1979).
17. A. V. Babkin, V. I. Kolpakov, V. N. Okhitin, and V. V. Selivanov, *Applied Mechanics of Continuous Media* (MGTU im. N. E. Baumana, Moscow, 2006), Vol. 3 [in Russian].
18. N. I. Koroteev and I. L. Shumai, *Physics of High-Power Laser Radiation* (Nauka, Moscow, 1991) [in Russian].
19. I. B. Delone, *Interaction of Laser Radiation with Matter* (Nauka, Moscow, 1989) [in Russian].
20. S. E. Kuratov, A. A. Serezhkin, and A. A. Chesnokov, http://chemphys.edu.ru/issues/2015-16-1/articles/316/.
21. S. I. Andreev, I. V. Verzhilovskii, and Yu. I. Dymshits, Sov. Tech. Phys. **15**, 1109 (1970).
22. I. Vladoiu, M. Stafe, C. Negutu, et al., U.P.B. Sci. Bull., Ser. A **70** (4) (2008).
23. Ya. B. Zel'dovich and Yu. P. Raizer, *Physics of Shock Waves and High-Temperature Hydrodynamic Phenomena* (Fizmatlit, Moscow, 2008; Academic Press, New York, 1966, 1967).
24. J. H. Tillotson, General Atomic Report GA-3216 (General Atomic, San Diego, CA, 1962).
25. R. T. Allen, Report GAMD-7834 (General Atomic, San Diego, CA, 1967).
26. A. J. Ward, Master's Theses (Marquette Univ., Wisconsin, 2009).
27. A. K. Kapila, R. Menikoff, J. B. Bdzil, et al., Phys. Fluids **13**, 3002 (2001).
28. S. Xu and D. S. Stewart, J. Eng. Math., No. 31, 143 (1997).
29. A. K. Kapila, D. W. Schwendeman, J. B. Bdzil, et al., Combust. Theory Model. **2**, 781 (2007).
30. E. L. Lee and C. M. Tarver, Phys. Fluids **23**, 2362 (1980).
31. Yu. P. Khomenko, A. N. Ishchenko, and V. Z. Kasimov, *Numerical Modeling of Interior Ballistic Processes in Barrel Systems* (SO RAN, Novosibirsk, 1999) [in Russian].
32. G. I. Kanel', S. V. Razorenov, A. V. Utkin, et al., *Shock Wave Phenomena in Condensed Systems* (YaKUS-K, Moscow, 1996) [in Russian].
33. J. A. Saenz and D. S. Stewart, J. Appl. Phys., No. 104, 043519 (2008).
34. A. Amsden, H. Ruppel, and W. Hirt, Report LA-8095, UC-32 (Los Alamos Sci. Laboratory, 1980).
35. A. A. Samarskii and Popov, Yu. P., *Application of Difference Methods to Problems of Gas Dynamics* (Nauka, Moscow, 1992) [in Russian].
36. N. G. Bourago and V. N. Kukudzhanov, Mech. Solids **40**, 35 (2002).
37. S. Kubota, T. Saburi, Y. Ogata, et al., AIP Conf. Proc. **1426**, 231 (2012).

Translated by K. Gumerov